Optical Engineering

SPIEDigitalLibrary.org/oe

Telescopes for space-based gravitational wave missions

Jeffrey C. Livas
Petar Arsenovic
John A. Crow
Peter C. Hill
Joseph M. Howard
Lenward T. Seals
Shahram Shiri

Telescopes for space-based gravitational wave missions

Jeffrey C. Livas
Petar Arsenovic
John A. Crow
Peter C. Hill
Joseph M. Howard
Lenward T. Seals
Shahram Shiri
NASA Goddard Space Flight Center
8800 Greenbelt Road
Greenbelt, Maryland 20771
E-mail: Jeffrey.Livas@nasa.gov

Abstract. Space-based observation of gravitational waves promises to enable the study of a rich variety of high energy astrophysical sources in the 0.0001 to 1 Hz band using signals complementary to traditional electromagnetic waves. Gravitational waves represent the first new tool for studying the sky since gamma ray telescopes debuted in the 1970s, and we expect compelling science to be the result. The fundamental measurement is to monitor the path length difference between pairs of freely falling test masses with laser interferometry to a precision of picometers over gigameter baselines. The test masses are arranged in an equilateral triangle to allow simultaneous measurement of both gravitational wave polarizations. The heliocentric orbital space environment enables the test masses to be shielded from large ground motions at low frequencies, and allows the construction of long measurement baselines that are well matched to the signal wavelengths. Optical telescopes play an important role in the measurement because they deliver laser light efficiently from one spacecraft to another. The telescopes are directly in the measurement path, so there are additional performance requirements to support precision metrology beyond the usual requirements for good image formation. [DOI: 10.1117/1.OE.52.9.091811]

Subject terms: telescopes; interferometry; laser applications; metrology; space optics; astronomy.

Paper 130181SS received Feb. 1, 2013; revised manuscript received Jun. 17, 2013; accepted for publication Jun. 25, 2013; published online Jul. 31, 2013.

1 Introduction

The low frequency band (0.0001 to 1 Hz) of the gravitational wave spectrum has a rich collection of astrophysical sources. The laser interferometer space antenna (LISA)[1,2] has been the reference mission to cover this science for over 20 years. Although recently severe budget constraints have forced both the National Aeronautics and Space Administration (NASA) and the European Space Agency (ESA) to reformulate this joint mission concept at a lower cost point, the proposed missions still retain most of the LISA-like features and differ mainly in scale size and duration.[3,4] The five basic LISA-like features are (1) drag free test masses, (2) continuous laser ranging with frequency-stabilized lasers, (3) heliocentric spacecraft orbits, (4) million-kilometer separation baselines between spacecraft, and (5) time-delay interferometry for post-processing signal extraction. We call the class of such mission concepts space-based gravitational wave observatories (SGOs).

Space-based missions complement ground-based observatories such as LIGO, with its partners and collaborators,[5] and pulsar timing arrays.[6]

Although the situation is far from clear, it appears that the best near-term option for a space-based mission is the ESA Cosmic Visions Program call for an L2 mission.[7] ESA is currently leading a technology demonstration mission, LISA Pathfinder,[8] to demonstrate the drag-free technology that isolates the proof masses. Successful completion of the mission, currently scheduled to launch in 2015, will put gravitational wave science in a competitive position for L2. A consortium of European universities and national laboratories supported by their ESA member state national space agencies is developing a proposal for the L2 opportunity, eLISA (evolved LISA), based on the proposal submitted for the L1 call.[9] (The JUpiter ICy moon Explorer mission was ultimately selected for L1.) The immediate goal of telescope technology development in the US is to demonstrate a design that meets the requirements of the European-led mission by the middle of the decade for consideration as a possible US contribution to the mission. If eLISA is not selected, the work could be applied to a NASA-led mission in the next decade with only minor changes.

The motivation for this paper is to describe the performance needed from an optical telescope to enable the measurement of gravitational waves in space. Section 2 describes the requirements, including a discussion of both conventional specifications and two key special challenges of precision metrology. Section 3 discusses the design of the telescope, including optical, mechanical, materials, and systems issues. Section 4 describes some of the progress so far on demonstrating the two key challenges. Section 5 looks at the path forward, and the final section is a conclusion.

1.1 *Science*

Gravitational waves are generated by accelerating masses just as electromagnetic waves are generated by accelerating charges. The lowest order radiator is a time-changing quadrupole rather than a dipole as in electromagnetism.[10] The simplest time-changing quadrupole moment is a pair of masses in orbit around each another, and such sources are ubiquitous in the Universe.

The four basic sources of gravitational waves and the resulting science are summarized in Table 1 and discussed in more detail in the literature.[2,3,11–14] Every time a new

0091-3286/2013/$25.00 © 2013 SPIE

Table 1 Summary of main expected sources of gravitational waves and the resulting science.

Source	Description	Science
Massive black hole mergers (MBHM)	Follow million-solar-mass BHs as they spiral together and merge	Formation of large scale structure in the Universe
Extreme mass ratio inspirals (EMRI)	Follow solar-mass BHs as they spiral into a supermassive BH	Map the gravitational field of a black hole: precision test of GR
Ultra-compact galactic binaries	Half of visible stars in the galaxy are in binary systems	Stellar evolution, supernova type Ia progenitors
Unknown: cosmic strings? Cosmological background?	Discovery space: sources we cannot anticipate	New discoveries—probably the most exciting science

kind of telescope has been developed, the discovery space has proven far more interesting than the formal science case.

1.2 *Measurement System and the Role of the Telescope*

The basic measurement concept for any SGO is a strain in spacetime $\Delta L/L \sim 10^{-21}/\sqrt{\mathrm{Hz}}$. The strain measurement is made by making an interferometric measurement of the change in separation between proof masses over a long baseline. In practice this means measuring differential separations of order $10^{-12}\ \mathrm{m}/\sqrt{\mathrm{Hz}}$ over baselines of order 1 million km.

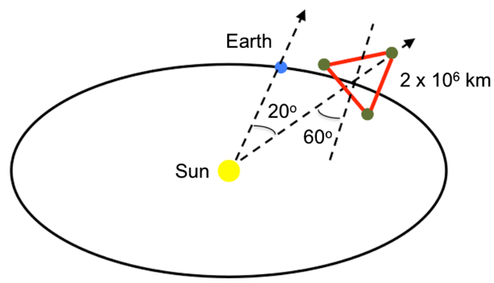

Fig. 1 Orbit and orientation of a typical SGO constellation. The plane of the triangle is tilted at 60 deg with respect to the ecliptic, and the triangle rotates about its center once per year as it orbits the Sun. Each spacecraft is in an independent Keplerian orbit, so no station-keeping is required.

The SGO is in the same basic orbit as the earth, with three spacecraft in independent Keplerian orbits forming a triangle in a plane inclined at 60 deg to the ecliptic. Independent orbits mean no formation flying or station-keeping is required to keep the triangular formation. The formation rotates about its center once per year, sweeping the antenna pattern across the sky. Figure 1 shows the orbit and the orientation of a typical constellation.

The telescope must deliver optical power efficiently to the detector on a far spacecraft, and it must maintain dimensional path length stability through the telescope to a level consistent with the displacement sensitivity noise budget. The telescope design must also minimize any coupling of pointing jitter to apparent displacement. Figure 2 shows a simplified diagram of the distance measurement between proof masses showing a pair of telescopes directly in the measurement path. Each telescope transmits a power of 1 W to the far spacecraft and simultaneously receives approximately 100 pW. A more detailed description of the instrumentation may be found in Ref. 15.

2 Requirements

The requirements for a telescope are taken from the proposal submitted to the ESA Cosmic Visions Program L1 program. This proposal is expected to be the model for the proposal to the L2 call, regarded as the most likely near-term opportunity

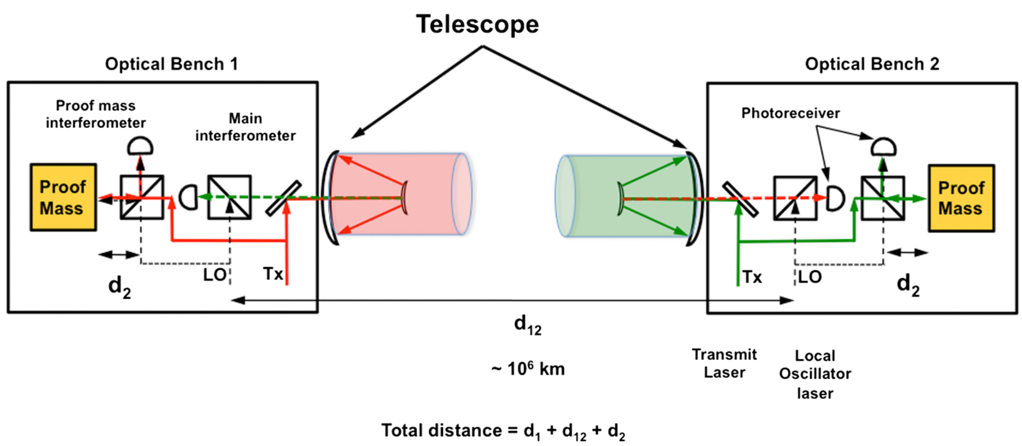

Fig. 2 Simplified diagram of the separation measurement between pairs of proof masses in different spacecraft to illustrate the role of the telescopes. The total distance measurement is made in three parts to simplify testing. Two parts are the measured distance from each proof mass to the nearby optical bench, a distance of ~20 cm. The third part is the distance from the optical bench in one spacecraft to the bench in the other, a distance of ~10^6 km. Two telescopes are directly in series with this measurement.

Table 2 Key requirements for a space-based precision metrology telescope. Requirements 6 and 10 are the most challenging.

	Parameter	Requirement driver	eLISA requirement
1	Wavelength		1064 nm
2	Wavefront quality over science field of view	Pointing	$\leq \lambda/30$ rms
3	Field-of-regard (spatial acquisition)	Acquisition time	± 200 mrad
4	Field-of-view (science)	Orbits	± 7 mrad out-of-plane[a] ± 4.2 mrad in-plane
5	Boresight accuracy	FOV, pointing	± 1 mrad
6	Telescope subsystem optical path length stability	Path length noise/pointing	$\leq 1\ \mathrm{pm}/\sqrt{\mathrm{Hz}} \times \sqrt{1+(\frac{0.003}{f})^4}$ where $0.0001 < f < 1$ Hz $1\ \mathrm{pm} = 10^{-12}$ m
7	Afocal magnification	Short arm interferometer	$200/5 = 40x(\pm 0.4)$
8	Mechanical length from primary mirror vertex	Spacecraft size	≤ 350 mm
9	Optical throughput	Shot noise	>0.85
10	Scattered light	Displacement noise budget	$<10^{-10}$ of transmitted power

[a]Out-of-plane or in-plane refers to the plane defined by the equilateral triangle of the SGO constellation. Spatial acquisition field of regard is the angular field over which the telescope must be able to receive a beacon signal for acquiring initial pointing. Full compliance with specifications is required only over the science FOV.

for a space-based gravitational wave mission. These requirements are summarized in Tables 2 and 3 and unless specifically referenced otherwise, are derived from Ref. 3. The main differences from the reference LISA mission are the diameter of the entrance pupil (400 mm for LISA) and the science field of view ($\pm 10\ \mu$rad for LISA). These differences are due to the smaller baselines and slightly different orbits of the eLISA mission and do not represent a relaxation of any basic performance specification. Requirements 6 and 10 are unusual, challenging, and specific to the precision metrology application. They are discussed in more detail below.

Table 3 shows the optical interface specifications for the telescope. Six identical telescopes are required for flight, plus a spare, and two or three for ground testing, for a likely total of about 10. The ideal design must be robust enough for small-scale manufacturing at this level.

2.1 *Conventional Specifications*

Most of the specifications for the telescope are similar to specifications for any imaging telescope, although the underlying driving requirement may be different. For example, we require $\lambda/20$ rms wavefront error of the entire system to

Table 3 Optical Interface specifications for the telescope.

	Parameter	Derived from	eLISA/NGO
Interfaces: received beam (entrance pupil)			
11	Stop diameter (D) (entrance pupil)	Noise/pointing	200 mm (± 2 mm)
12	Stop location (entrance pupil)	Pointing	Entrance of beam tube or primary mirror
Interfaces: telescope exit pupil			
13	Exit pupil location from primary vertex	Pointing	150 ± 20 mm (on axis) behind primary mirror[16]
14	Exit pupil diameter	Optical bench	5 mm (± 0.05 mm)
15	Exit pupil distortion	SNR	<10%
16	Exit pupil chief ray angle error		$\pm 50\ \mu$rad

maintain efficient power delivery on axis to the far spacecraft, which is proportional to the Strehl ratio of the telescope squared (one transmitting, one receiving). Of this system-level budget, $\lambda/30$ is allocated to the telescope, and the rest reserved for the optical bench and the laser source. Loss of power from the laser source through the telescope is specified separately by the throughput, which includes obscurations, but not the beam overlap contrast on the detector. The science field of view is the angular range over which full specifications must be maintained. Variation in the line-of-sight pointing is due to normal orbital motion and is outside the measurement band. The acquisition field of regard is a larger angular range chosen in combination with the uncertainty cone for attitude knowledge of the spacecraft to limit the time needed for acquiring closed loop pointing between pairs of telescopes.[17] The telescope need not meet the most challenging specifications over the field of regard.

2.2 *Special Challenges*

Two of the specifications present special challenges and will be described separately here.

2.2.1 *Dimensional stability*

The most unusual requirement for the telescope is the optical path length stability (Table 2 requirement 6). Optical path length is the net total path length through the telescope as experienced by either the transmitted or received beam from input pupil to exit pupil and can be defined as the accumulated phase divided by the wave number ($2\pi/\lambda$), where λ is the design wavelength, 1064 nm. The path length stability is important over times compatible with the measurement bandwidth of 0.1 to 0.0001 Hz, or 10 to 10,000 s. The absolute value is less important in part because we plan to include a focus adjustment as part of the design.

The requirement is specified as the amplitude power spectral density of path length variations through the telescope that can be tolerated in the overall noise budget for the interferometer metrology system.

Although the path length stability requirement is straightforward to test in principle, it requires careful experimental technique. Section 4.1 discusses the challenges and progress in more detail.

2.2.2 *Stray light*

The stray light requirement is a consequence of two main contributing factors. First, there is simultaneous transmit and receive through the same telescope. For a communications system this is called "full duplex" operation. In this context, it means that a high power (~1 W) continuous (CW) transmit beam is coming from the optical bench out of the large telescope aperture at the same time that a low power signal (~100 pW continuous, or one part in 10^{-10} of the transmitted signal) is being received from the far spacecraft.

Second, the received signal is detected coherently. That means the science signal is extracted by mixing the incoming signal with a local oscillator laser and square-law detecting the term cross-product term. This is a very sensitive detection scheme because it allows a small incoming signal to create an interference signal with a much higher power local reference laser beam, but it also means that the detector is very sensitive to stray light.

Stray light may be represented as a single electric field vector at the detector that represents the (vector) sum of all the stray light from the optical system, including reflections from the transmitted beam, the optical bench, and anything else (see Fig. 3). In general, the electric field may take several reflections to make it to the detector, so the amplitude of the field is small with respect to the electric field strength of the local oscillator laser, but the phase relationship is unknown and may be changing as the reflecting surfaces move. The power on the photo-receiver, which represents the square of the total electric field incident on the detector, contains a cross-term that has the product of the electric fields of the local oscillator laser E_{lo} and the stray light e and the cosine of the angle between the two fields $\delta\theta$:

$$\begin{aligned} P_{\mathrm{det}} &= |\vec{E}_{\mathrm{lo}} + \vec{E}_{\mathrm{total}}|^2 = E_{\mathrm{lo}}^2 + E_{\mathrm{total}}^2 + 2\vec{E}_{\mathrm{lo}} \cdot \vec{E}_{\mathrm{total}} \\ &= P_{\mathrm{lo}} + P_{\mathrm{total}} + 2\vec{E}_{\mathrm{lo}} \cdot (\vec{E} + \vec{e}) \\ &= P_{\mathrm{lo}} + P_{\mathrm{rec}} + 2E_{\mathrm{lo}}E\cos(\varphi_{\mathrm{rec}}) + 2E_{\mathrm{lo}}e\cos(\delta\theta). \end{aligned} \tag{1}$$

The phase relationship between the stray light and the local oscillator is determined by the path length of the stray light as it travels to the detector. If the path length is stable, then the angle $\delta\theta$ is fixed, and the stray light contribution is simply a background level. More generally, the phase angle will change and the stray light contributes a time-varying signal that appears as an unwanted modulation in addition to the desired signal φ_{rec}. The ratio of the cross-product terms is the ratio of unwanted scattered light modulation to signal, and is given by the ratio of the field strengths e/E multiplied by the ratio of the cosines of the variation in phase angles. Although the general expression can be quite complicated, it should be clear why there is a tight requirement on both path length stability and the fraction of the transmitter power that can be scattered.

2.3 *Manufacturability*

The instrument design to detect gravitational waves requires six flight telescopes that are nominally identical. For most imaging telescopes, even a very challenging design can be made to work by tweaking during ground testing because only one copy is constructed. With multiple copies, it is essential to be able to routinely construct the telescopes to meet the required tolerances and specifications, in order to minimize schedule risk and to incur only recurring engineering costs.

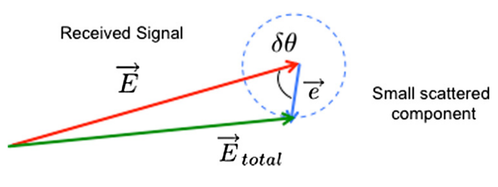

Fig. 3 The total electric field on the detector is the vector sum of the received signal and any scattered light. Scattered light on the detector may have an unknown and changing phase relationship with the signal, resulting in an undesirable modulation of the total electric field.

3 Design

The telescope design for the LISA baseline mission may be adequately satisfied by a near diffraction-limited classical Cassegrain-style optimized three-mirror anastigmat system—either on-axis or off-axis. A Cassegrain-style design is easy to manufacture and has good off-axis performance. However, the gravitational wave application is for a precision length measurement system, not an imaging system, so the motivations for some of the requirements are slightly different and may lead to different design choices.

3.1 *Trade-Off/Issues*

An off-axis design would normally be the preferred choice to meet the scattered light specification because the lack of a central obstruction increases the optical efficiency and reduces stray light effects. However, a preliminary tolerance analysis indicates that the straightforward optical design (next section) is very difficult to build in a normal optical shop. This is a problem because we need six flight units and several for ground testing—approximately 10 telescopes total. A robust design is necessary to be sure that the fabrication of the telescopes is not an undue schedule risk, and also to allow the telescopes to be interchangeable.

In addition, the expected thermal environment has both an axial and a transverse temperature gradient, so environmental effects would naturally tend to create off-axis aberrations. An on-axis design generally has better resistance to these environmental effects, but the on-axis spot in the center of the secondary mirror causes unacceptably high levels of scattered light. Therefore, the best design choice is not clear and requires further work. Table 4 summarizes the various design considerations. If it can be shown that the on-axis design can meet the scattered light requirements, or that an off-axis design is robust and can be readily fabricated, then the choice may become clear. A study is currently in progress to resolve these issues.

3.2 *Optical Design*

The basic optical design for the telescope is an optimized Cassegrain-style afocal three-element anastigmat. Figure 4(a) shows a ray tracing of a nominal 20-cm aperture on-axis Cassegrain design suitable for the proposed eLISA mission. The right-hand image [Fig. 4(b)] shows an off-axis Cassegrain design with the same optical prescription as in the left-hand image. The pair of mirrors on the right-hand side of both designs functions as a collimating lens and is mounted rigidly on a translation stage to allow adjustment of the focus. This degree of freedom will allow at least partial compensation for any shifts in the telescope alignment that occur in the process of moving from a room temperature ground environment to a zero-g space environment at the operating temperature. No transmissive elements are used to avoid the temperature dependence of the index of refraction. The optical bench may have some transmissive elements, so the goal is to keep the path length stability budget as low as possible for the telescope to reserve margin for the rest of the optics. The variation of optical path length with field angle (or solid-body rotation) is higher with an on-axis design than with an off-axis design, but in general these variations should occur slowly and be outside the measurement band. If necessary, they may be calibrated out.

Table 4 Summary of the main design trade-offs between and on-axis and an off-axis telescope.

Design	WFE with temperature gradient	Scattered light	Manufacturability (need 10)
On-axis	+	−	+
Off-axis	−	+	−

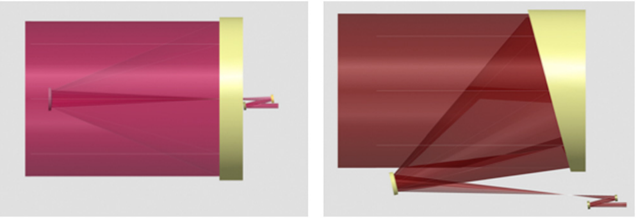

(a) (b)

Fig. 4 (a) On-axis telescope design based on a 3-mirror anastigmat. The pair of mirrors to the right of the primary mirror function as a collimating lens implemented with reflecting surfaces. The exit pupil is located on the right-hand side 150 mm behind the primary mirror vertex per requirement 15, Table 3 for the interface with the optical bench. (b) Off-axis version with the same nominal optical prescription. The exit pupil meets the same requirement as for the on-axis design but displaced vertically. The vertical displacement will be accommodated by changing the optical bench design.

3.3 *Wavefront Error*

The main requirements are that power is delivered efficiently on axis in the far field, and that the path length remains stable. An rms wavefront error allocation of $\lambda/30$ will meet these requirements. The optical efficiency specification includes obscuration losses, but does not include the beam overlap visibility. See Secs. 2.1 and 3.5 for more discussion.

3.4 *Stray Light*

The stray light specification is challenging and will require measurements to be sure we understand all the contributions. We believe that an off-axis design will have better performance, but the key question is whether an on-axis design can be made to work well enough. The design study currently under way is examining a number of strategies for reducing light reflected on axis from the secondary mirror including anti-reflection or absorbing coatings, petaled masks similar to those designed for coronagraphs, or even a hole.

3.5 *Risks*

The main technical risk identified today beyond stray light and dimensional stability is contamination. The stray light performance is driven by contamination of the telescope optics rather than surface roughness, so it will be important to keep the optics clean during the testing of the telescopes, and then the integration and test phase with the spacecraft, a task which may take up to 2 years. A further risk is that the telescope may well be one of the coldest surfaces in the spacecraft, so some care must be taken to make sure that the optics do not function as a getter and actually pump contaminants. Verification of the telescope dimensional stability is a potential risk since it is a challenging measurement.

3.6 *Mechanical*

There are several mechanical challenges. We need to keep the envelope of the entire package small so as not to drive the size of the spacecraft. We also need to mount the optical bench rigidly to the telescope but allow a temperature gradient so as to keep the optical bench near room temperature but allow the telescope to sit at $\sim -70°C$ (see discussion in Sec. 3.4). This requires a stiff mounting structure that also acts as a thermal insulator.

We have identified a candidate compact actuator for the focus mechanism based on a commercially available piezoelectric translation stage that clamps when not in motion. Adjustment of the focus is expected to be a set-and-forget operation that occurs during initial commissioning and then again during regularly scheduled engineering maintenance operations once or twice per year only if necessary. A sensitivity analysis of the telescope optical design indicates that the effect of the focus mechanism on the dimensional stability is at least one order of magnitude below the required stability of the telescope.

3.7 *Materials*

One of the keys to maintain optical path length stability is the proper choice of materials. The thermal environment of the spacecraft is extremely stable. The solar array sees a constant illumination that walks around the normal to the array once per year at an angle of 30 deg. Modeling predicts that the thermal fluctuations at the optical bench will be $\sim 10^{-6}$ K$/\sqrt{\text{Hz}}$ level in the measurement band with appropriate passive thermal isolation.

Although the fluctuations in the temperature are extremely low, there are large static thermal gradients both along the axis of the telescope and transverse to it. The axial gradient occurs because the secondary mirror is looking at (cold) space, and the primary mirror is located near the optical bench, which must be held near room temperature to take advantage of the low coefficient of thermal expansion of Zerodur. The transverse gradient arises naturally because the solar array faces the sun and the bottom deck of the spacecraft faces space. There may also be a concentration of electronics located between the two telescopes on a spacecraft. These static thermal gradients complicate the design of the telescope for optical path length stability. The standard athermal design methodology where a structure is made to maintain image quality as the temperature varies over some specified range usually assumes that the structure is all at or near the same temperature. We can approximate that assumption by choosing a material with a very high thermal conductivity to "short out" the gradient. For a composite material, thermal modeling predicts axial temperature gradients on the order of 70 K, with a ~ 10 K transverse gradient. For silicon carbide, the models predict gradients of about 1.5 K axial and <1 K transverse (Fig. 5). The transverse gradient, if not properly planned for in the design, has the potential to distort the structure and introduce off-axis aberrations that cannot be corrected with focus. Furthermore, an athermal telescope maintains image quality but does not necessarily keep the optical path length constant. The telescope design must do both to meet the requirements for this application.

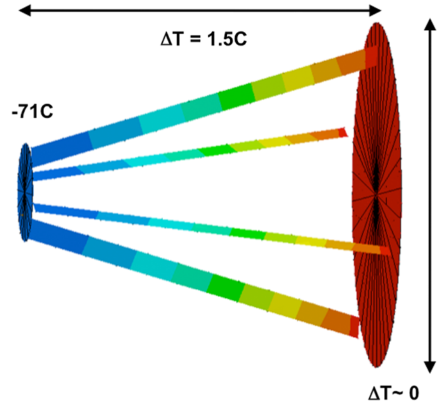

Fig. 5 Modeled temperature distribution of the telescope metering structure of silicon carbide. A composite material structure model showed axial gradients of ~70°C and transverse gradients of 10°C.

Single crystal silicon is a candidate material because it has thermal and mechanical properties similar to SiC at room temperature that improve for this application at lower temperatures. It is also possible to make very good and lightweight mirrors from a single crystal silicon.

Composite materials have been widely studied because it is possible to tailor their properties through the choice of materials and construction methods, but some initial studies of optical path length stability have shown that water absorption in composite materials can lead to continuous long-term "creep" or dimensional changes in the material that can affect our ability to perform a measurement.[18,19] This is a concern but does not rule out the material yet. The use of composites may introduce some schedule risk and/or additional cost if the materials must be kept bagged and purged when not in use, and if additional time must be allowed for them to outgas under vacuum before performance testing.

3.8 *System*

There are a number of system level design considerations. First, it is important to keep the telescope afocal so that the interface between the optical bench and the telescope is a collimated beam. This relaxes the tolerance on the distance between the bench and the telescope. It is also important to have a real exit pupil that can be relayed to the main science detector so that there is a minimum beam walk caused by the known angular pointing jitter.

As the spacecraft orbits the Sun, the geometry of the triangular constellation changes, and in particular, the line-of-sight pointing of the telescopes can change by as much as ± 0.6 deg. For the baseline reference LISA mission, the entire optical assembly consisting of a telescope, and optical bench, and the proof mass assembly were pivoted with respect to the spacecraft to maintain the pointing. If the angular variation can be reduced, either by a different choice of orbit or by applying a periodic correction to the orbits to maintain the angles to ± 0.1 deg, it is possible to consider replacing the motion of the entire telescope by a mirror that rotates as a part of the telescope design. The rotating mirror must produce an angle change with minimum piston, so it is a challenging design. If it can be implemented, it will enable a simplified design for the optical assembly, eliminate an articulation mechanism and possibly a launch lock, and allow us to eliminate a potentially risky optical fiber link[20] between the optical benches on the different arms of the same spacecraft. This moveable mirror option is referred to as "in-field guiding" and is currently under study.

4 Progress/Measurements

4.1 *Dimensional Stability*

As part of the development work on the telescope, we constructed a prototype on-axis metering structure to maintain the primary to secondary mirror distance out of silicon carbide. We chose silicon carbide to avoid the outgassing problems with carbon fiber reinforced plastic composites,[18] and to avoid temperature gradients expected under the anticipated operating environments. Figure 6 shows a photograph of the structure. It has four legs so that the shadow of the structure has four symmetric elements that match the symmetry of the main quadcell detector. A four-legged structure is mechanically over-constrained, so future designs may support the secondary mirror differently (e.g., off-axis).

Figure 7 shows the results of measurements with the prototype silicon carbide structure showing that it is possible, at least in principle, to make a metering structure with the required stability.[21] The red curve shows that the metering structure closely follows the temperature fluctuations at frequencies below ∼4 mHz. On-orbit the temperature fluctuations are expected to be roughly 100 times lower than in the test chamber, so the structure should meet the requirement. The challenge is to build a complete telescope, both the structure and the optics, with the required stability. Silicon carbide should work, and single-crystal silicon looks like a good candidate. Our experience with composites has not been as good.[18,19] Other groups have made measurements

Fig. 6 Prototype silicon carbide metering structure constructed to test dimensional stability. Two small (1 in. dia) high reflectivity mirrors were attached to both the top and bottom plate to form a Fabry–Perot resonator for testing. Height is approximately 600 mm.

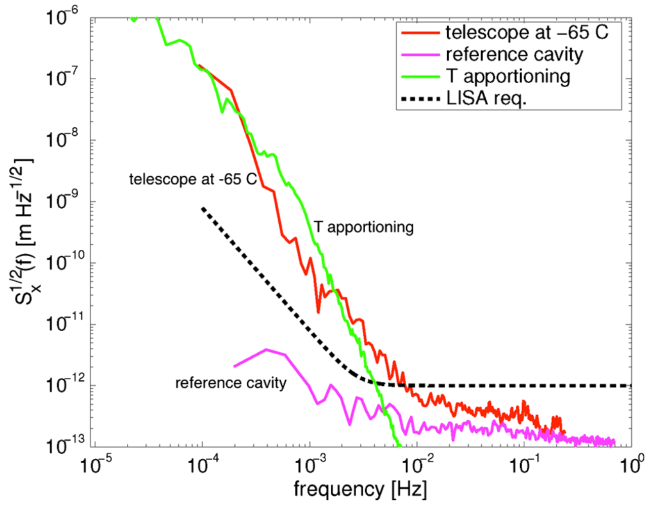

Fig. 7 Measured results of the dimensional stability of the structure in Fig. 6 as inferred from the frequency fluctuations of a laser locked to the Fabry–Perot resonator. The black-dotted line shows the requirement for the telescope. The lowest curve (magenta) shows the stability of the reference cavity. The red curve shows the telescope spacer structure, which exceeds the requirement below about 0.01 Hz. The green curve shows the dimensional stability expected from the measured thermal fluctuations, indicating that the performance is limited by these fluctatuations. On orbit thermal fluctuations are expected to be a factor of 100 lower.

with composites with different results,[22,23] but no one has succeeded in meeting all the requirements simultaneously with a realistic design yet.

4.2 *Stray Light*

A stray light analysis has been started using the commercial nonsequential ray-tracing package FRED.[24] The analysis has focused on developing a model of the on-axis eLISA telescope, including obstructions, based on the optical prescription and a mechanical model, plus some simplified assumptions for surface roughness and cleanliness for materials and coatings. We used a preliminary design for the eLISA optical bench courtesy of the University of Glasgow[16] to define approximate locations for the detectors and field stops. The preliminary results show a scattered light power of 6×10^{-11} W (60 pW) on the detector for 1 W transmitted to the sky, and we expect a further reduction if polarization is taken into account. This level of stray light is below the expected 100 pW received signal from the far spacecraft, so it is approaching the right order of magnitude, but the simulation does not yet include all the expected contributions.

The initial stray light assessment for the telescope design suggests that the performance of a telescope will be limited by surface contamination rather than surface roughness, as discussed earlier in the section on risks. It is expected the stray light performance of an off-axis design will be better than that of an on-axis telescope with the secondary mirror reflection suppressed simply because rays traced through the off-axis system tend to be reflected from surfaces with larger angles and hence lower stray light. However, it will be important to verify these expectations experimentally to be sure that it is possible to achieve the low levels in practice. Calculations and preliminary measurements[25,26] have shown that special apodized masks similar to those used for planet finding interferometers can be used to suppress reflections to roughly the required levels.

5 Path Forward

Many of the telescope requirements have been met with proof-of-concept demonstrations or with subsystems such as a metering structure or a mock-up of a secondary mirror. The challenge going forward is to assemble a complete prototype telescope that meets all the performance requirements. We are currently working with an industrial contractor to develop a design for a telescope that addresses the scattered light requirement and the manufacturability issues outlined in Table 4. We plan to choose a design approach based on the results and then fabricate a prototype and verify compliance with the requirements by testing. We also plan to experimentally investigate options for suppressing stray light as a check on the modeling results.

6 Conclusion

Telescopes for space-based precision measurement applications such as gravitational wave detection present some unique challenges not usually found in telescopes designed for more conventional imaging applications. These challenges are: high precision dimensional stability over measurement times of up to 10,000 s, very low stray and scattered light performance, and a robust design that can be easily and quickly replicated.

Acknowledgments

The authors would like to thank P. Bender, G. Mueller, J. Sanjuan, A. Spector, and the members of the Gravitational Wave Study Team for support and stimulating discussions. They would also like to thank the referees for detailed suggestions for improving the manuscript. This work is supported in part through NASA Grant 11-SAT11-0027 NNH11ZDA001N "Research Opportunities in Space and Earth Sciences" (ROSES-2011) for Strategic Astrophysics Technology (SAT).

References

1. P. Bender and K. Danzmann, and LISA Study Team, "LISA for the detection and observation of gravitational waves," Max-Planck-Institut fur Quantenoptik, Garching Technical Report No. MPQ233, 1998, http://lisa.gsfc.nasa.gov/Documentation/ppa2.08.pdf (11 July 2013).
2. LISA assessment study report (Yellow Book), ESA/SRE(2011)3, http://sci.esa.int/science-e/www/object/index.cfm?fobobjectid=48364 (11 July 2013).
3. NGO assessment study report (Yellow Book), ESA/SRE(2011)19, http://sci.esa.int/science-e/www/object/index.cfm?fobobjectid=49839 (11 July 2013).
4. Gravitational-Wave Mission Concept Study Final Report, http://pcos.gsfc.nasa.gov/physpag/GW_Study_Rev3_Aug2012-Final.pdf (11 July 2013).
5. LIGO Scientific Collaboration: Partner experiments and collaborations, http://www.ligo.org/partners.php (11 July 2013).
6. G. Hobbs, "Pulsar timing arrays: status and techniques," in *Proc. IAU Symposium*, J. van Leeuwen, Ed., Vol. 291, pp. 165–170 (2012).
7. http://sci.esa.int/Call-WP-L2L3 (11 July 2013).
8. LISA Pathfinder overiew, http://www.esa.int/esaSC/120397_index_0_m.html (11 July 2013).
9. http://www.elisa-ngo.org (11 July 2013).
10. B. Schutz, "Gravitational waves on the back of an envelope," *Am. J. Phys.* **52**(5), 412–419 (1984).
11. P. Amaor-Seoane et al., "Low-frequency gravitational-wave science with eLISA/NGO," *Class. Quant. Grav.* **29**(12), 124016 (2012).
12. P. Amaro-Seoane et al., "Intermediate and extreme mass-ratio inspiral astrophysics, science applications, and detection using LISA," *Class. Quant. Grav.* **24**(17), R113–R169 (2007).
13. S. Nissanke et al., "Gravitational-wave emission from compact Galactic binaries," *Astrophys. J.* **758**(2), 131 (2012).
14. A. Stroeer and A. Vecchio, "The LISA verification binaries," *Class. Quant. Grav.* **23**(9), S809–S817 (2006).
15. O. Jennrich, "LISA technology and instrumentation," *Class. Quant. Grav.* **26**(15) 153001 (2009).
16. E. W. Fitzimons and H. Ward, private communication, Institute for Gravitational Research, School of Physics and Astronomy, University of Glasgow, Glasgow, UK G12 8QQ.
17. P. Maghami et al., "An acquisition control for the laser interferometer space antenna," *Class. Quant. Grav.* **22**(10), S421–S428 (2005).
18. J. Sanjuan et al., "Carbon fiber reinforced polymer dimensional stability investigations for use on the laser interferometric space antenna mission telescope," *Rev Sci. Instrum.* **82**(12), 124501 (2011), http://link.aip.org/link/?RSI/82/124501.
19. A. Preston, "Stability of materials for use in space-based interferometric missions," Ph.D. Dissertation, University of Florida (2010).
20. R. Fleddermann et al, "Measurement of the non-reciprocal phase noise of a polarization maintaining single-mode fiber," *J. Phys. Conf. Ser.* **154**(1) 012022 (2009).
21. J. Sanjuan et al., "Note: silicon carbide telescope dimensional stability for space-based gravitational wave detectors," *Rev. Sci. Instrum.* **83**(11), 116107 (2012).
22. A. L. Verlaan et al., "LISA telescope assembly optical stability characterization for ESA," *Proc. SPIE* **8450**, 845003 (2012).
23. J. C. Machado et al., "Picometer resolution interferometric characterization of the dimensional stability of zero CTE CFRP," *Proc. SPIE* **7018**, 70183D (2008).
24. FRED non-sequential ray tracing software, http://www.photonengr.com/software/ (11 July 2013).
25. A. Spector and G. Mueller, "Back-reflection from a Cassegrain telescope for space-based interferometric gravitational-wave detectors", *Class. Quant. Grav.* **29**(20), 205005 (2012).
26. S. Shiri and W. Wasylkiwskyj, "Poisson-spot intensity reduction with a partially transparent petal-shaped optical mask," *J. Opt.*, **15**(3), 035705 (2013).

Jeffrey C. Livas earned an SB in physics in 1981 and a PhD in physics in 1987, both from the Massachusetts Institute of Technology. He joined the NASA Goddard Space Flight Center in 2005 to work on the laser interferometer space antenna (LISA) Project. His research interests include gravitational wave detection and data analysis, precision measurement, and optical communications.

Petar Arsenovic earned a BA in mathematics from Johns Hopkins University in 1984, an MS in mechanical and aerospace sciences from the University of Rochester in 1985, and a PhD in materials science and engineering from Johns Hopkins University in 1992. He joined the NASA Goddard Space Flight Center in 1988 and currently serves as a Technologist and Associate Head of the Optics Branch.

John A. Crow earned a BA in mechanical engineering at the Johns Hopkins University in 1995. He has been at NASA Goddard Space Flight Center since 1985. He is currently a mechanical systems engineer on the James Webb Space Telescope Integrated Science Instrument Module.

Peter C. Hill earned a SB in pure mathematics from the University of Texas, Austin in 2002, and an MS in optical engineering at the University of Arizona in 2006. He has worked at NASA Goddard since 2009 as an optical analyst. His current research interests are stray light analysis and novel materials for mirror fabrication.

Joseph M. Howard earned a PhD in optics from the University of Rochester in 1999. Since 1999, he has been at the NASA Goddard Space Flight Center. He currently serves as the James Webb Space Telescope Lead Optical Designer, and conceived and manages the optical design lab (ODL), an optics branch facility that applies concurrent engineering principles to the optical design process.

Lenward T. Seals is currently working at the NASA Goddard Space Flight Center. His current research interest is in optical system design and stray light analysis. He earned a PhD degree in applied physics from the Georgia Institute of Technology in 2001.

Shahram Shiri earned SB and MS degrees from Louisiana Tech University, and a PhD from George Washington University. Since 1996, he as worked at NASA Goddard Space Flight Center on a number of missions and is currently working on system validation and optical analysis of wavefront sensing and control algorithms for the James Webb Space Telescope. His current research interests include the design and fabrication of petaled occultation masks for coronagraph and stray light reduction applications.